

Governors State University

OPUS Open Portal to University Scholarship

All Capstone Projects

Student Capstone Projects

2021

Bond Valence Sum Analysis for Determination of Oxidation States in Coordination Compounds

Dreyvon McCray

Follow this and additional works at: <https://opus.govst.edu/capstones>

For more information about the academic degree, extended learning, and certificate programs of Governors State University, go to http://www.govst.edu/Academics/Degree_Programs_and_Certifications/

Visit the [Governors State Analytical Chemistry Department](#)

This Capstone Project is brought to you for free and open access by the Student Capstone Projects at OPUS Open Portal to University Scholarship. It has been accepted for inclusion in All Capstone Projects by an authorized administrator of OPUS Open Portal to University Scholarship. For more information, please contact opus@govst.edu.

**Bond Valence Sum Analysis for Determination of Oxidation States in Coordination
Compounds**

By

Dreyvon McCray

B.S., Governors State University, 2018

Capstone Project

Submitted in partial fulfillment of the requirements

For the Degree of Master of Science,

With a Major in Analytical Chemistry



Governors State University

University Park, IL 60484

2021

Advisor: Dr. Kulugamma Gedera Sanjaya Ranmohotti

CAPSTONE APPROVAL FORM

WE, THE UNDERSIGNED MEMBERS OF THE COMMITTEE,
HAVE APPROVED THIS CAPSTONE PROJECT

**Bond Valence Sum Analysis for Determination of Oxidation States in Coordination
Compounds**

By

Dreyvon McCray

COMMITTEE MEMBERS

K.G. Sanjaya Ranmohotti, Ph.D. (Chair)
Chemistry

Joong- Won Shin, Ph.D.
Chemistry

Walter Henne, Ph.D.
Chemistry

Governors State University
University Park, IL 60484

May 2021

Acknowledgments

This work would not be possible without the support of the chemistry committee at Governors State University. The student was grateful for all of those with whom he has had the pleasure to work with during this time in other related projects. Each member of the committee has provided me with guidance, both personal and professional. Nobody has been more supportive of me for pursuing this milestone of this project than God, the members of my family, and friends. I would like to thank my parents for showing me love and guidance in whatever I pursue. They are the ultimate role models. I would also like to acknowledge X-Ray Facilities and Capabilities at Clemson university and this center provides access to the Cambridge Structural Database, the Inorganic Crystal Structure Database, and the Powder Diffraction File.

TABLE OF CONTENTS

Abstract.....	6
Introduction.....	7
Calculation Section.....	18
Results and Discussion.....	20
Conclusion.....	37
References.....	38

List of Figures

- Figure 1.** Partial structure showing the arrangement ions in NaCl. The Na⁺ ions are shown in white and Cl⁻ ions are shown in blue (left). Bond fluxes in the (110) plane of TiO₂ (right).....9
- Figure 2.** Partial structure showing MnO₅ unit22
- Figure 3.** Partial structure showing Mn₂O₅ unit.....23
- Figure 4.** Partial structure showing Mn₃O₅ unit.....24
- Figure 5.** Partial structure showing phosphorous-centered oxygen tetrahedra.....25
- Figure 6.** The barium cation resides in a BaO₆ environment.....27
- Figure 7.** The partial structure showing potassium ions residing in the middle of Mn₆(PO₄)₆ units and barium ions residing in between the Mn₆(PO₄)₆ units (left). The Mn₆(PO₄)₆ unit together with barium cations capping both sides to form a cage for potassium ions to reside in (right).28
- Figure 8.** Coordination environment around potassium cations.....29
- Figure 9.** The corner-sharing PO₄ tetrahedra and MnO₅ square pyramids form a pseudo one dimensional channel structure with two type of channels where barium and potassium cations reside in one channel while rubidium cation sitting in the other.....30
- Figure 10.** Drawings of RbO₈ polyhedra. The dotted lines represent long Rb-O bonds.....32
- Figure 11.** The representations of the unit cell of the compound showing a space-filling representation which reveals the regular arrangements of Ba, Rb, K, Mn, P, and O atoms in three dimensions where the metal lattice arrange themselves in a certain pattern which can be represented as a 3D box structure. The Ba ions are shown in green, Rb ions are shown in gray, K ions are shown in light green, Mn ions are shown in blue, P ions are shown in yellow, and the O ions are shown in red. There are four types of sites in the unit cell: central, face, edge, and corner positions.....35

List of Tables

Table 1. Atomic coordinates and equivalent displacement parameters for title compound.....	19
Table 2. Crystallographic Data for title compound	20
Table 3. Selected Bond Distances (\AA) and Angles (deg) in MnO_5 unit, and Bond valence sum.....	22
Table 4. Selected bond distances (\AA) and angles (deg) in Mn_2O_5 unit, and bond valence.....	23
Table 5. Selected bond Distances (\AA) and angles (deg) in Mn_3O_5 unit, and bond valence sum.....	24
Table 6. Selected Bond Distances (\AA) in PO_4 units and Bond valence sum.....	25
Table 7. Selected Bond Distances (\AA) in BaO_6 units and Bond valence sum.....	27
Table 8. Selected Bond Distances (\AA) in KO_6 units and Bond valence sum.....	29
Table 9. Selected Bond Distances (\AA) in RbO_9 units and Bond valence sum.....	32
Table 10. The summery of Bond valence sum	33
Table 11. Number of atoms per unit cell in title compound.....	36

Abstract

Transition metal ions in coordination compounds very often adopt different oxidation states. The Bond Valence Sum (BVS) model, based solely on structural information, relates the bond lengths around a metal center to its oxidation state. This model can provide a reliable information on the oxidation states of the metal ions and serves as an additional support for the accuracy of crystal structure determination so that BVS analysis through the comparison of the observed bond distances with reliable crystallographic data, it is possible to validate the empirical formula. Transition metal ions in coordination compounds can adopt different oxidation states. The most interesting nature of the manganese complexes is the ability to adopt different oxidation states of manganese which can adopt 3-, 2-, 1-, 0, 1+, 2+, 3+, 4+, 5+, 6+ and 7+ oxidation state. We applied the fundamental concept of the BVS method and summarize the empirical BVS parameters for selective metal ions that have more than one oxidation state. In the crystal structure that was selected to analyze, we found that the bonds of alkali atoms bonded to oxygen were significantly longer than those reported for other inorganic compounds. Therefore, our interest was in exploring whether the oxidation state of the atoms in this structure could be calculated from the bond distances to validate the crystal structure determination. The final values resulted from Bond-valence sum (BVS) calculations for the title compound can be summarized as +1.93, +1.94, +1.91, +4.95, +4.99, +2.02, +1.87, +1.14, and +1.03 valence units for Mn(1), Mn(2), Mn(3), P(1), P(2), P(3), Ba(1), Ba(2), Rb(1), and Rb(2), respectively, which in each case is close to the expected values of 2 for Mn, 5 for P, 2 for Ba, and 1 for Rb.

Introduction

The Bond Valence Sum henceforth BVS method has been used by several research groups to estimate the oxidation states of metal ions in compounds containing transition-metal (TM) oxides. Although the BVS¹, appears to be extremely useful to coordination chemists, it has not been utilized routinely. It is well known fact that transition metal ions in coordination compounds can adopt different oxidation state.² The BVS model, based solely on structural information, relates the bond lengths around a metal center to its oxidation state. This model can provide details on the oxidation states of the metal ions and serves as an additional support for the accuracy of crystal structure determination.³ Before discussing BVS model in detail, a brief overview of valence, oxidation number, and coordination number will be presented.

The terms such as “valence” (or valency), oxidation state (or oxidation number), and coordination number have all been in use for decades in both elementary and advanced chemistry texts. However, a cursory perusal of the recent literature reveals inconsistencies of usage that are likely to confuse students, instructors, and researchers.⁴ Therefore it is essential to get clarified the notions of valence, oxidation number, and related concepts such as “formal charge”, and coordination number. The word “valence” (also called “valency”) has a plethora of uses, as illustrated by the phrases “valence electrons”, “valence bond theory”, “valence shell electron pair repulsion theory (VSEPR)”, and “bond-valence model”.⁵ In general, the valence of an atom in a molecule is equal to the difference between (i) the number of valence electrons in the free atom (i.e., the group valence, N) and (ii) the number of nonbonding electrons on the atom in

the molecule; (valence = number of electrons in valence shell of free atom – number of nonbonding electrons on atom in molecule). Basically valence refers to number of electrons that an atom uses in bonding. Oxidation number is defined as The charge remaining on an atom when all ligands are removed heterolytically in their closed form, with the electrons being transferred to the more electronegative partner where homonuclear bonds do not contribute to the oxidation number. Formal charge is refers to The charge remaining on an atom when all ligands are removed homolytically. The coordination number is defined as The number of atoms bonded to the atom of interest. The valences of atoms in simple compounds can be illustrated using a simple approach. For example, the number of electrons in valence shell (N) of nitrogen atom in NH_3 is 3 and the number of nonbonding electrons is 2 so that nitrogen atom in NH_3 has a valence of 3, an oxidation of -3, 3 bonds and a coordination number of 3.

The bond valence model not only preserves many of the traditional concepts of chemistry, such as atom, bond, cation, anion, electronegativity and valence, but also gives them precise definitions. model gives a complete description of the Coulomb field, including the repulsive electrostatic forces between like charged ions and the long-range interactions that make the two-body potential model computationally intensive. Both of these effects are correctly described by the localized bonds of the bond valence model. Before discussing these in detail, a brief historical sketch will be presented.

In 1911, it has been shown that the sodium atom in crystals of sodium chloride has six nearest chlorine neighbors. This model led to the rethinking the contemporary model of chemical bonding that held that the number of chemical bonds formed by an

atom was equal to its atomic valence. An alternative model for describing inorganic compounds was therefore developed by Born, Lande', and Madelung.⁶ According to them sodium atoms were considered as cations carrying a single positive charge and that the chlorine atoms were be considered anions carrying a single negative charge and they introduced a repulsive potential to keep the atoms apart where the equilibrium state of such a system is one in which each cation is surrounded by anions and each anion is surrounded by cations as observed in the crystal structure of NaCl as shown in Figure 1.

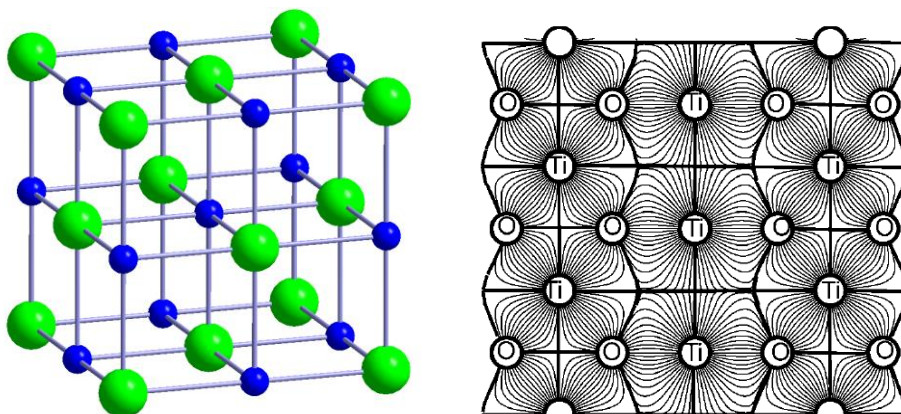


Figure 1. Partial structure showing the arrangement ions in NaCl. The Na^+ ions are shown in blue and Cl^- ions are shown in light green (left). Bond fluxes in the (110) plane of TiO_2 (right).

Although the subsequent development of quantum mechanics has shown that this ionic model is an unrealistic description of chemical bonding, the model has proved to be remarkably robust and successful in describing chemical structure specially the arrangement of atoms so that even though it did not give a good description of the physical forces that bind the atoms into solids and liquids, it was used to make good predictions of the positions the occupancy of the ions.

In 1929 using this ionic model, Pauling⁷ analyzed a number of the mineral structures that had been determined during the previous decade and proposed his much-quoted five rules governing the structures of minerals. The most important of these is the second rule, the *principle of local charge neutrality*. According to this rule the negative charge, V_a on each anion is neutralized by the positive charges on its neighboring cations. He assigned to each bond a *Pauling bond strength*, S_p , given by eq 1.

$$S_p = V_c / N_c \quad (1)$$

where V_c is the valence (i.e. formal charge) of the cation and N_c is its coordination number, that is the number of first neighbor anions that surrounded the cation. According to his electrostatic valence rule, eq 2, the sum of the bond strengths received by each anion tends to compensate the valence of the anion.

$$V_a = \sum S_p \quad (2)$$

This rule implies that in order to provide local charge neutrality, the cations and anions arrange themselves in a systematic way. This idea was expressed in a more visual form by Bragg et al.⁸ who suggested that the electric field could be represented by Faraday's lines of field (electrostatic flux) and that the observed arrangements of ions in a crystal corresponds to an arrangement that keeps the field lines as short as possible. A picture of the flux lines lying in the (110) plane of rutile (TiO_2) is shown in Figure 1.⁹ Today we recognize that Pauling's bond strength and Bragg's electric flux lines were early attempts to estimate what we currently called the bond valence; the limitation of the technology of structure determination at that time did not allow for a better definition so that eq 2 is usually only approximately true.¹⁰ It was not until the 1950s and 1960s that the ionic

model could be further developed with the aid of the newly available computers that could calculate the potential energy of every atom pair in the crystal. During that time, with the improvement in the quality of crystal structure determination, Baur has suggested that there was a strong correlation between the length of a bond and Pauling's concept of its strength.¹¹ Eventually the term *bond Valence* was introduced by Donnay et al. in order to describe a bond strength derived from its measured bond length, utilizing the term *Pauling bond strength* to refer to the estimate of the bond valence derived from the coordination number using eq 1.¹² When they summed around the anions and cations, the bond valences were found to reproduce the atomic valences (ionic charges) much more accurately the Pauling bond strengths.^{13,14} Determination of this correlation for different bond types and the discovery that these correlations can be transferable between different crystals, the bond valence model provided a more quantitative picture of chemical structure than was possible with Pauling's second rule.

The bond valence model describes the structures of compounds containing bonds between atoms of different electronegativity. In each bond, the atom with the smaller electronegativity is called the cation and that with the larger electronegativity is called the anion. The valences, V , of cations and anions have been derived from the observed stoichiometries of compounds taking into account the fact that this satisfy the electroneutrality principle.

$$\sum V_i = 0 \quad (3)$$

where the sum is over all atoms in the formula unit. In practice, this means that the cation valence is equal to the number of its valence-shell electrons used in bonding (often called

the formal oxidation state) and the anion valence is the negative of the number of holes in the valence shell. Cations are therefore assigned a positive valence and anions are assigned a negative valence.

Speaking of the theoretical basis of the bond valence sum model, a derivation from an approximate electron density model has been introduced by Mohri.¹⁵ He has assumed that each bond involves the same number of electrons and that the valence of a bond is proportional to its electron density. He has divided the number of electrons by the volume they occupy, taken to be proportional to the cube of the bond distance after those parts of the distance that lie within the atom cores have been subtracted. Using the sum of the cation radii, r , as a measure of the sizes of the cores, the space occupied by the bonding electrons is $(R - r)^3$, where R is the bond length. This has led to eq 4.

$$s/s' = (R - r)^3 / (R' - r)^3 \quad (4)$$

where s is the valence of a bond of length R and s' is the valence of a bond of length R' . He shows that this equation can be reduced to eq 5 which is commonly used to describe the bond-valence-bond-length correlation.

$$S = \exp((R_0 - R)/b) \quad (5)$$

where S is the experimental bond valence, R the observed bond length, and R_0 and b are fitted bond Valence parameters. R_0 represents the nominal length of a bond of unit valence and it depends on the sizes of the atoms forming the bond. On the other hand, b measures the softness of the interaction between the two atoms. Equation 5 is now the most widely used relation, and an accumulated table of values of R_0 and b can be obtained from the literature.¹⁶ The bond-valence R_0 and b parameters are typically

obtained by fitting equation 5 to a set of trusted structures, and will vary with the element types and oxidation states of atoms.¹⁰ In most circumstances, a value of $b = 0.37 \text{ \AA}$ provides satisfactory results and we assume this value throughout, although the need to adjust b in some circumstances has been acknowledged.¹⁰ Today many researches still use reference literature values for bond-valence (R_0) parameters, which were derived two decades ago from manually curated structures and extrapolated linear relationships between bond-valence contributions.^{17,18} Following the initial publication of bond-valence parameters based on inorganic crystal structures numerous studies have discussed the bond-valence model in the context of small-molecule crystal structures in the Cambridge Structural Database(CSD)^{19,20} as well as in the Inorganic Crystal Structure Database (ICSD)²¹. Some notable results based on CSD data include bond-valence parameters for copper²² and lanthanides.^{23,24} (2009). Mohri has derived the bond-valence-bond-length correlation shown in eq 6 from his bonding electron density model.¹⁵

$$S = S_0 [(R_0 - r)/(R - r)]^3 \quad (6)$$

where r is the sum of the cation and anion core radii, which has taken to be the same as the Shannon ionic radii.^{25,26} S_0 is a reference bond valence and R_0 the corresponding bond length. This expression is based on identifying the bond valence with a notional calculation of the electron density in the bond region. It has been proposed a method for determining the van der Waals radii for transition metals by assuming that any interatomic distance that corresponds to a valence of 0.01 vu would represent a van der Waals interaction.²⁷ They (Nag et al.) have used Pauling's van der Waals radii for the

anions, combined with the bond lengths predicted for bonds of 0.01 vu, to calculate van der Waals radii for all the d block elements.

The bond-valence model relies on the notion that the length of a bond between atoms depends on its valence, i.e. the number of electron pairs forming the bond or the electrostatic flux between participating atoms. Another guiding idea, which follows from the above definition, is the bond-valence sum (BVS) rule, which states that the valences of the bonds of an atom should sum up to its oxidation state (which we denote S).²⁸ One may express mathematically and utilize the bond length–valence correlation by adopting various expressions and testing them empirically. Out of many attempts to establish a function for the prediction of the valence through the sum of all the bond lengths, it was not until 1985 when Brown et al.¹⁷ proposed a general expression shown in eq 7

$$V_{ij} = \sum S_{ij} = \sum \exp[(R_0 - r_{ij})/b] \quad (7)$$

where V_{ij} is the oxidation state of atom I , S_{ij} is the bond valence and r_{ij} is the length of the bond formed between atoms i and j . The bond-valence R_0 and b parameters are typically obtained by fitting this expression to a set of trusted structures, and will vary with the element types and oxidation states of atoms i and j . The exponential form cited above has the convenient property that the optimal bond-valence parameter b is relatively insensitive to the atom type and binding partners.¹⁷ As mentioned above in most circumstances, a value of $b = 0.37 \text{ \AA}$ provides satisfactory results.²⁹ The sum of the individual values of S_{ij} for the j bonds around a central metal gives the BVS, which is generally close to the formal oxidation state of the metal. For instance, if one applies the

BVS to a metal ion in the +2 oxidation state, the sum of all its bond valences will lead to a value close to the integer two. The same calculation applied with R_0 parameters for other oxidation states will also provide a V value close to the integer two, however with a considerable discrepancy. This model can be applied to any coordination environment regardless of the coordination number. In fact, a metal ion with the same oxidation state will generally display longer bonds with an increase in coordination number. The empirical values of R_0 have been calculated and reported for many metal-ligand combinations and different oxidation states.^{18,29,30} A number of programs are available for calculating bond valences.³¹ The Web site SoftBV³² provides an introduction to bond valences and gives the user an opportunity to check a structure in SHELX or CIF format. VaList³³ is another program that calculates bond valences and bond valence sums for a list of bond lengths supplied by the user in CIF, GSAS or FULLPROF format.

Bond valence sum analysis provide an excellent, and often the only way to assign oxidation states, especially for mixed valence compound. Shields et al.³⁴ have tested the ability of bond valences to automatically assign oxidation states to metal ions in the structures of complexes found in the Cambridge Structural Database.³⁵ They have reported a success rate of 88% in a test sample of four-coordinate Cu complexes. The BVS analysis is useful for interpreting Extended X-ray absorption fine structure (EXAFS) data on metalloproteins where bond lengths have been determined with high precision but where coordination numbers were usually not uniquely defined in the fit.³⁶ By determining how many multiples of S_{ij} for each type of bond are required to give the formal oxidation state, the coordination number can also be determined.^{37,38}

Transition metal ions in coordination compounds can adopt different oxidation states. Various types of transition metal (TM) oxides are constructed through the condensation of metal (M) centered MO_6 octahedra by sharing their vertices, edges or faces.³⁹ The most interesting nature of the inorganic chemistry of manganese complexes is the ability to adopt different oxidation states of manganese. Complexes have been prepared that contain manganese in the 3-, 2-, 1-, 0, 1+, 2+, 3+, 4+, 5+, 6+ and 7+ oxidation state.⁴⁰ Since the manganese ion is flexible enough to adapt a variety of valence states, it can possess different kinds of magnetic moments depending on its usual high-spin valence states ($S = 5/2, 2,$ and $3/2$ for $\text{Mn}^{2+}, \text{Mn}^{3+}$ and Mn^{4+} , respectively). The bond valence sum approach, which predicts the average oxidation state of metals in a transition metal compound according to their metal-oxygen bond lengths and empirically determined parameters, has correctly predicted oxidation states in a variety of well characterized manganese based oxide compounds.⁴¹ The determination of BVS typically requires as the first step, the compilation of a database of reliable reference crystal structure data. In our work the main source was the Crystallographic Information File (CIF) of unpublished crystal structure containing metal (Mn) centered MnO_5 polyhedra. It is well known fact that the most common use of the BVS approach is to validate the crystal structure determinations by comparing the valences of the atoms with the sums of their experimental bond valences so that discrepancy between the atomic valences and bond valences sums draws the attention to possible misassignments of the cation valence and this is a possible indication that there is a problem with the assumed model of the structure. In the crystal structure that was selected to analyze, we found that

the bonds of alkali atoms bonded to oxygen were significantly longer than those reported for other inorganic compounds. Therefore, our interest was in exploring whether the oxidation state of the atoms in this structure could be calculated from the bond distances to validate the crystal structure determination. Good agreement between the calculated and postulated oxidation states would provide support for the chemical formula and the accuracy of a crystal structure determination. However, if the oxidation state calculated from the bond distances obtained from a crystal structure differs markedly from the postulated chemical formula, usually there is a problem in the crystal structure determination. This is somewhat challenging task taking into account the fact that manganese tends adopt multiple oxidation states. Basically an oxidation state is presumed for the manganese ion (II or III) and the bond valences are calculated for each bonded atom for each presumed oxidation state. The bond valence values are then summed to give an estimate of the oxidation state. If this estimate matches that of the assumed oxidation state, then the oxidation can be assigned to that which is assumed. If the estimate does not match that of any assumed oxidation state, then some other interpretation about the structure may be appropriate, such that the structure determination is not valid, there is a non-integral oxidation state, there are significant steric interactions, etc. Notwithstanding these ambiguity, here I show that the BVS method is surprisingly accurate to estimate oxidation states in transition metal oxides and these calculations can be performed by hand or using a few lines of code on a minimal calculator.

Calculation Section

The bond length data for BVS calculation were acquired from the Crystallographic Information File (CIF) where the structure refinement which has been aided by software packages and the used package of software was the SHELXL program suite⁴² and the refinement was based on F^2 by least-squares, full-matrix techniques. Generally, the results of the structure refinement yield a list of x,y,z assignments for each atom in the unit cell, the distance of the nearest atomic neighbors and shape of the anisotropic intensity center for each atom (thermal parameters). The atomic coordinates and the thermal parameters are listed in Table 1 and selected bond distances and angles are listed in Tables 3 to 6. Table 2 reports the crystallographic data of the title compound. By using structural parameters such as unit cell, space group, and atomic positions, the crystal structure was drawn using *Diamond-2.1*,⁴³ which is a user-friendly molecular and crystal structure visualization software. As shown in Table 2, The X-ray single-crystal structural analysis shows that this phase crystallizes in a trigonal space group with $a = 15.873(2) \text{ \AA}$, $b = 8.555(2) \text{ \AA}$, $\gamma = 120^\circ$, and $V = 1866.7(5) \text{ \AA}^3$; $P\bar{3}$ (No. 147); $Z = 2$. The crystal structure of the title compound can be described as three-dimensional architecture containing pseudo one dimensional channels. The corner-sharing PO_4 tetrahedra and MnO_5 square pyramids form two type of pseudo one dimensional channels where barium and potassium cations reside in the bigger channel while rubidium cations occupy in the smaller channel.

Table 1. Atomic Coordinates and Equivalent Displacement Parameters for the title compound

Atom	Wyckoff notation	x	y	z	Uiso (Å ²) ^a
Ba(1)	1a	0	1.00000	1.00000	0.0161(3)
Ba(2)	2d	1/3	2/3	1.5369(1)	0.0150(3)
Rb(1)	6g	0.36052(6)	1.00205(6)	1.52020(9)	0.0097(3)
Rb (2)	6g	0.3018(2)	0.9959(1)	0.9795(2)	0.0145(4)
K (1)	2d	1/3	2/3	1.9580(7)	0.045(2)
K(2)	6g	0	1.00000	1.50000	0.043(2)
Mn(1)	6g	0.10695(9)	0.9075(1)	1.3588(2)	0.0138(4)
Mn(2)	6g	0.4312(1)	0.8660(1)	1.1674(2)	0.0138(4)
Mn(3)	6g	0.2406(1)	0.4709(1)	1.8664(2)	0.0132(4)
P(1)	6g	0.4614(2)	0.8986(2)	1.7752(3)	0.0119(5)
P(2)	6g	0.4423(2)	1.2366(2)	1.7432(3)	0.0119(5)
P(3)	6g	0.1028(2)	0.8749(2)	1.7432(3)	0.0134(5)
O(1)	6g	0.4751(5)	0.6800(5)	1.3497(8)	0.022(1)
O(2)	6g	0.4760(5)	0.9967(5)	1.2864(8)	0.019(1)
O(3)	6g	0.4523(5)	1.1459(5)	1.7451(9)	0.024(2)
O(4)	6g	0.2131(5)	0.8689(5)	1.3240(9)	0.027(2)
O(5)	6g	0.3548(5)	0.8716(5)	1.7639(9)	0.024(2)
O(6)	6g	0.2788(5)	0.8248(5)	1.0883(8)	0.020(1)
O(7)	6g	0.1853(6)	0.9806(5)	1.7343(9)	0.032(2)
O(8)	6g	0.1708(5)	0.6522(5)	1.6778(8)	0.019(1)
O(9)	6g	0.1481(5)	1.0132(5)	1.1712(8)	0.025(2)
O(10)	6g	0.1854(5)	0.3248(5)	1.8273(8)	0.021(1)
O(11)	6g	0.4924(5)	0.8911(5)	0.9443(8)	0.020 (1)
O(12)	6g	0.2297(5)	1.0649(5)	1.4231(8)	0.021(1)

^a Equivalent isotropic U defined as one third of the trace of the orthogonalized U_{ij} tensor.

Table 2. Crystallographic Data for the title compound

Formula weight (amu)	1332.31
Crystal System	Trigonal
Space group	<i>P</i> -3 (No. 147)
a, (Å)	15.873(2)
c, (Å)	8.555(2)
γ , (°)	120
V, (Å ³)	1866.7(5)
Formula units, Z	3
Density, Calculated	3.551 g/cm ³

Results and Discussion

There are three crystallographically independent manganese atoms in this compound and all of them are coordinated to five oxygens to form distorted square pyramids. As shown in Figures 2-4, Mn(1), Mn(2), and Mn(3) adopt bond distances normally observed in the Mn²⁺. The Mn-O bond distances range from 2.057 Å to 2.371 Å and the average Mn-O distances in Mn(1)-O, Mn(2)-O and Mn(3)-O are 2.15 Å, 2.15 Å and 2.16 Å respectively. These are comparable with 2.11 Å, the sum of the Shannon crystal radii^{25,26} for five coordinated Mn²⁺ (0.89 Å) and three-coordinated O²⁻ (1.22 Å). In order to provide additional proof for this point and to eliminate the possibility of the occurrence of a Mn³⁺ ion, the BVS calculation was performed with the Mn-O bond lengths obtained from the crystal structure, R_0 values extracted from Table 3 for Mn^{II} and Mn^{III}, and b was set equal to 0.37. An example of the calculation of the valence for the bond Mn(1)-O(7)^{ix} (bond length $r_{\text{Mn(1)-O(7)}^{\text{ix}}} = 2.064 \text{ \AA}$) is as follows:

In the case of Mn^{II}, $R_0 = 1.790$, $s = \exp[(R_0 - r_{\text{Mn}(1)-\text{O}(7)}^{ix})/b] = 0.48$

In the case of Mn^{III}, $R_0 = 1.760$, $s = \exp[(R_0 - r_{\text{Mn}(1)-\text{O}(7)}^{ix})/b] = 0.44$

Similar calculations can be performed for other Mn-O bonds. The sum of the valences of the bonds around the Mn ion provide an estimation of its oxidation state. The result of the BVS calculations for Mn(1) is summarized in Table 3. The sum of bond valences is 1.93 v.u. for Mn^{II} and 1.78 v.u. for Mn^{III} and these values are closer to the integer two. Thus, it is reasonable to assign that the Mn(1) ion is in +2 oxidation state. The bond valence sum analysis^{17,18} also indicate that the formal oxidation state of manganese is Mn²⁺ as shown in Table 4 and 5 where the bond valence sum calculations on Mn(2)O₅ and Mn(3)O₅ give the values of +1.94 v.u. and +1.91 v.u., respectively.

The three phosphorous atoms are part of PO₄ tetrahedra (Figure 4), with P—O bond lengths ranging from 1.522(7)–1.561(7) Å (Table 1). The average P—O bond length (1.537 Å) in the title compound is close to 1.52 Å, sum of the Shannon crystal radii^{25,26} for four-coordinate P⁵⁺ (0.31 Å) and two-coordinate O²⁻ (1.21 Å). The bond valence sum (BVS) calculations^{17,18} based upon observed bond distances are consistent with the assigned formal oxidation states of the phosphate cations. To provide additional support for this estimation and rule out the possibility of the presence of an uncommon P³⁺ ion, the BVS calculation was also performed with the P-O bond lengths obtained from the crystal structure, R_0 values extracted from Table 6 for P^{III} and P^V, and b was set equal to 0.37.

Table 3. Selected Bond Distances (Å) and Angles (deg) in MnO₅ unit, and Bond valence sum

Bond	Bond length (Å)	Valence	
		Mn ^{II}	Mn ^{III}
Mn(1)-O(7) ^{ix}	2.064(8)	0.48	0.44
Mn(1)-O(4)	2.081(7)	0.45	0.42
Mn(1)-O(12) ^{ix}	2.116(7)	0.41	0.38
Mn(1)-O(9)	2.174(7)	0.35	0.33
Mn(1)-O(12)	2.339(7)	0.23	0.21
	Sum	1.93	1.78

O(4)-Mn(1)-O(12) ^{ix}	92.8(3)	O(7) ^{ix} -Mn(1)-O(12)	160.7(3)
O(7) ^{ix} -Mn(1)-O(9)	99.7(3)	O(4)-Mn(1)-O(12)	89.0(3)
O(4)-Mn(1)-O(9)	98.4(3)	O(12) ^{ix} -Mn(1)-O(12)	103.9(2)
O(12) ^{ix} -Mn(1)-O(9)	164.0(3)	O(9)-Mn(1)-O(12)	65.2(2)

Mn(1)O₅ Square pyramid

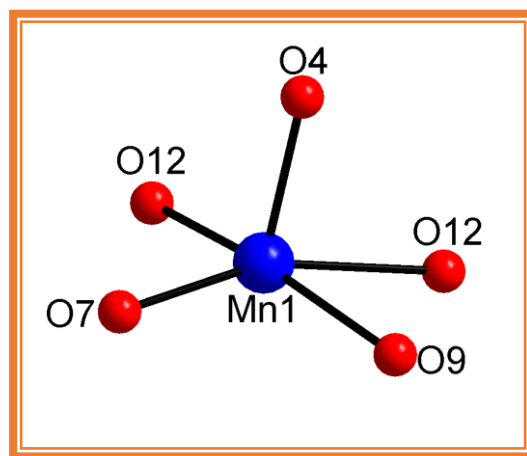


Figure 2. Partial structure showing MnO₅ unit (ball and stick drawing).

Table 4. Selected Bond Distances (Å) and Angles (deg) in MnO₅ unit, and Bond valence sum

Bond	Bond length (Å)	Valence	
		Mn ^{II}	Mn ^{III}
Mn(2)-O(11)	2.087(7)	0.45	0.41
Mn(2)-O(3) ^x	2.088(7)	0.45	0.41
Mn(2)-O(2)	2.091(7)	0.44	0.41
Mn(2)-O(1) ^{vii}	2.197(7)	0.33	0.31
Mn(2)-O(6)	2.271(7)	0.27	0.25
	Sum	1.94	1.79

O(11)-Mn(2)-O(3) ^x	89.8(3)	O(2)-Mn(2)-O(1) ^{vii}	87.1(3)
O(11)-Mn(2)-O(2)	111.1(3)	O(11)-Mn(2)-O(6)	96.3(3)
O(3) ^x -Mn(2)-O(2)	92.2(3)	O(3) ^x -Mn(2)-O(6)	160.8(3)
O(11)-Mn(2)-O(1) ^{vii}	157.6(3)	O(2)-Mn(2)-O(6)	102.4(3)
O(3) ^x -Mn(2)-O(1) ^{vii}	102.7(3)	O(1) ^{vii} -Mn(2)-O(6)	66.2(2)

Mn(2)O₅ Square pyramid

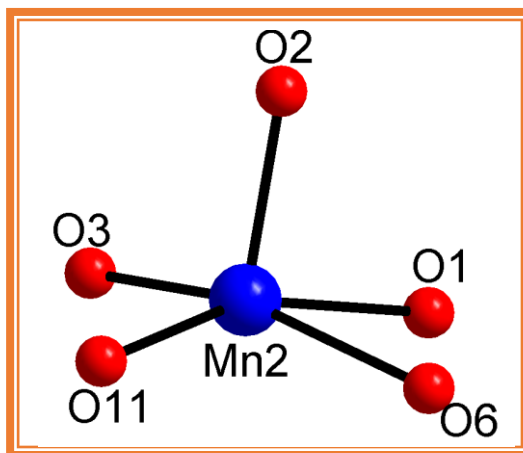


Figure 3. Partial structure showing MnO₅ unit (ball and stick drawing).

Table 5. Selected Bond Distances (Å) and Angles (deg) in MnO₅ unit, and Bond valence sum

Bond	Bond length (Å)	Valence	
		Mn ^{II}	Mn ^{III}
Mn(3)-O(10)	2.057(7)	0.48	0.45
Mn(3)-O(5) ^{vii}	2.080(7)	0.46	0.42
Mn(3)-O(6) ^{xv}	2.115(7)	0.41	0.38
Mn(3)-O(8) ^{vii}	2.187(7)	0.34	0.31
Mn(3)-O(11) ^{xvii}	2.371(7)	0.21	0.19
	Sum	1.91	1.76

O(10)-Mn(3)-O(5) ^{vii}	97.8(3)	O(10)-Mn(3)-O(6) ^{xv}	95.6(3)
O(5) ^{vii} -Mn(3)-O(6) ^{xv}	90.1(3)	O(10)-Mn(3)-O(8) ^{vii}	95.1(3)
O(5) ^{vii} -Mn(3)-O(8) ^{vii}	102.2(3)	O(5) ^{vii} -Mn(3)-O(11) ^{xvii}	161.1(3)
O(6) ^{xv} -Mn(3)-O(8) ^{vii}	162.4(3)	O(6) ^{xv} -Mn(3)-O(11) ^{xvii}	99.8(2)
O(10)-Mn(3)-O(11) ^{xvii}	97.1(3)	O(8) ^{vii} -Mn(3)-O(11) ^{xvii}	65.0(2)

Mn(3)O₅ Square pyramid

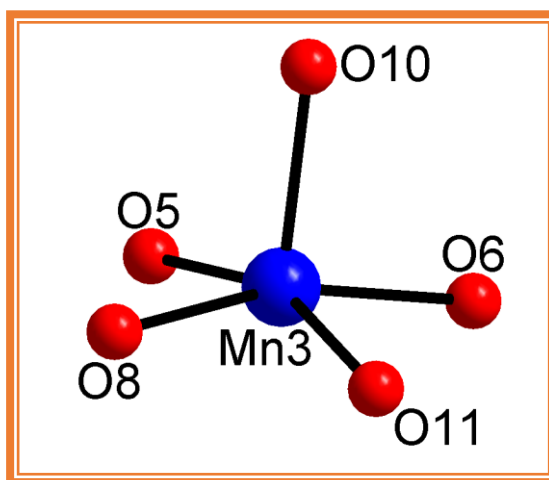
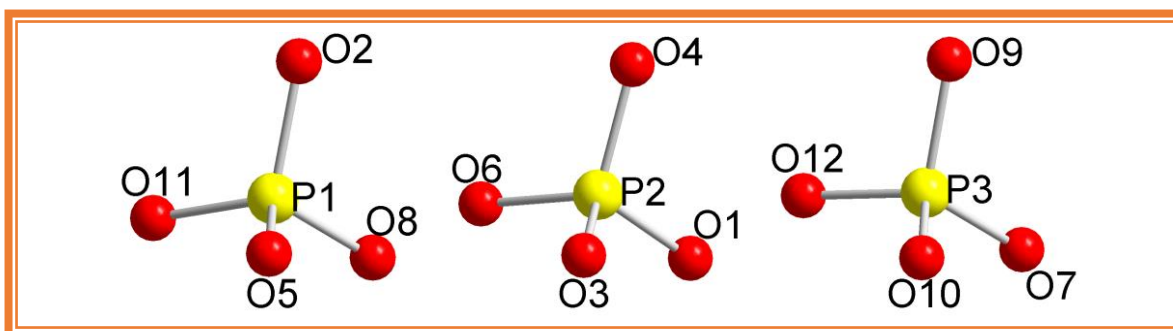


Figure 4. Partial structure showing MnO₅ unit (ball and stick drawing).

Table 6. Selected Bond Distances (Å) in PO₄ units and Bond valence sum

Bond	Bond length (Å)	Valence	
		P ^{III}	P ^V
P(1)-O(5)	1.525(7)	1.33	1.28
P(1)-O(8) ^{viii}	1.536(7)	1.29	1.24
P(1)-O(2) ^x	1.541(7)	1.27	1.23
P(1)-O(11) ^{xvi}	1.552(7)	1.23	1.19
	Sum	5.12	4.95
P(2)-O(4) ^{xi}	1.522(7)	1.34	1.29
P(2)-O(3)	1.526(7)	1.32	1.28
P(2)-O(1) ^x	1.539(7)	1.28	1.23
P(2)-O(6) ^{xi}	1.561(7)	1.20	1.16
	Sum	5.15	4.97
P(3)-O(10) ^{viii}	1.526(7)	1.32	1.28
P(3)-O(7)	1.528(7)	1.32	1.27
P(3)-O(9) ^{ix}	1.536(7)	1.29	1.24
P(3)-O(12) ^{ix}	1.551(7)	1.23	1.19
	Sum	5.17	4.99

P(1)O₄, P(2)O₄, and P(3)O₄ Tetrahedra**Figure 5.** Partial structure showing phosphorous-centered oxygen tetrahedra.

An example of the calculation of the valence for the bond P(1)-O(5) (bond length r P(1)-O(5) = 1.525(7) (Å) is as follows:

For the case of P^{III}, $R_0 = 1.63$, $s = \exp[(R_0 - r \text{ P(1)-O(5)})/b] = 1.33$

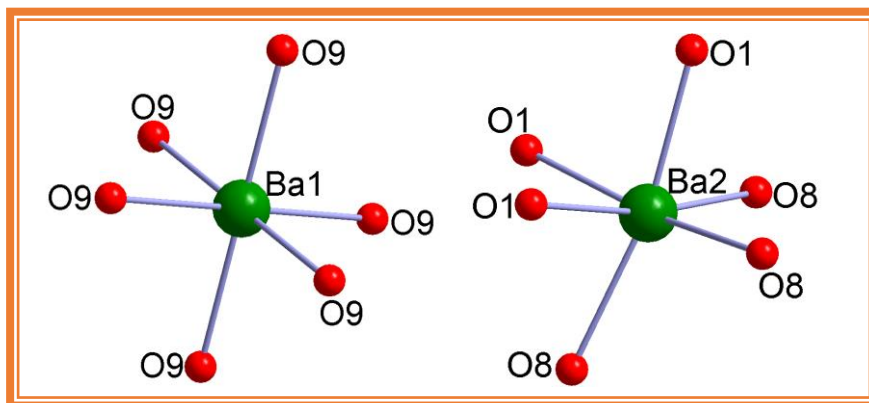
For the case of P^V, $R_0 = 1.617$, $s = \exp[(R_0 - r \text{ P(1)-O(5)})/b] = 1.28$

Similar calculations can be done for other phosphorous-oxygen bonds. The sum of the valences of the bonds around the P ion provide an estimation of its oxidation state. The result of the BVS calculations is summarized in Table 6. The sum of bond valences is 5.12 v.u. for P^{III} and 4.95 v.u. for P^V in P(1)O₄ tetrahedra and these values are closest to the integer five. The bond valence sum (BVS) calculations^{17,18} based upon observed bond distances are consistent with the assigned formal oxidation states of the other cations; the calculated valences for P(2)⁵⁺ and P(3)⁵⁺ cations are +4.97 v.u. and +4.99 v.u., respectively as shown in Table 6. Thus, we can agree with the fact that all the phosphorous ions in this compound are in +5 oxidation states.

Two crystallographically different barium cations are found in this compound. The barium cations reside in an irregular BaO₉ geometry, which can be seen in Figure 6. The average Ba-O distances in Ba(1)-O and Ba(2)-O are 2.69 Å and 2.71 Å respectively, which are comparable with the sum of Shannon crystal radii (2.70 Å) of six coordinate Ba²⁺ (1.49 Å) and O²⁻ (1.21 Å).^{25,26} The bond valence sum (BVS) calculations^{17,18} based upon observed distances are consistent with the assigned formal oxidation states of the cations; the calculated valences for Ba²⁺(1) and Ba²⁺(2) cations are +2.02 v.u. and +1.87 v.u., respectively as shown in Table 7.

Table 7. Selected Bond Distances (Å) in BaO₆ units and Bond valence sum

Bond	Bond length (Å)	Valence Ba ^{II}
Ba(1)-O(9) ⁱ	2.688(7)	0.34
Ba(1)-O(9)	2.688(7)	0.34
Ba(1)-O(9) ⁱⁱ	2.688(7)	0.34
Ba(1)-O(9) ⁱⁱⁱ	2.688(7)	0.34
Ba(1)-O(9) ^{iv}	2.688(7)	0.34
Ba(1)-O(9) ^v	2.688(7)	0.34
Sum		2.02
Ba(2)-O(1) ^{vii}	2.683(7)	0.34
Ba(2)-O(1) ^{viii}	2.683(7)	0.34
Ba(2)-O(1)	2.683(7)	0.34
Ba(2)-O(8)	2.751(7)	0.28
Ba(2)-O(8) ^{viii}	2.751(7)	0.28
Ba(2)-O(8) ^{vii}	2.751(7)	0.28
Sum		1.87

Ba(1)O₆ and Ba(2)O₆ Polyhedra**Figure 6.** The barium cation resides in a BaO₆ environment.

As shown in Figure 7, the $\text{Mn}_6(\text{PO}_4)_6$ units stack on top of each other along c -axis having barium cations in between them. K(2) cation resides in the middle of $\text{Mn}_6(\text{PO}_4)_6$ units formed by Mn(1)O₅ square pyramids whereas K(1) cation resides in the middle of $\text{Mn}_6(\text{PO}_4)_6$ unit formed by alternating Mn(2)O₅ and Mn(3)O₅ square pyramids. The barium cations residing front and back side of $\text{Mn}_6(\text{PO}_4)_6$ unit cap the bangle to form a cage. As shown in Figure 8, the average K-O distances in K (1)-O and K (2)-O are 3.30 Å and 3.32 Å respectively, which are significantly longer than the sum of Shannon crystal radii (2.73 Å) of six coordinate K⁺ (1.52 Å) and O²⁻ (1.21 Å).^{25,26}

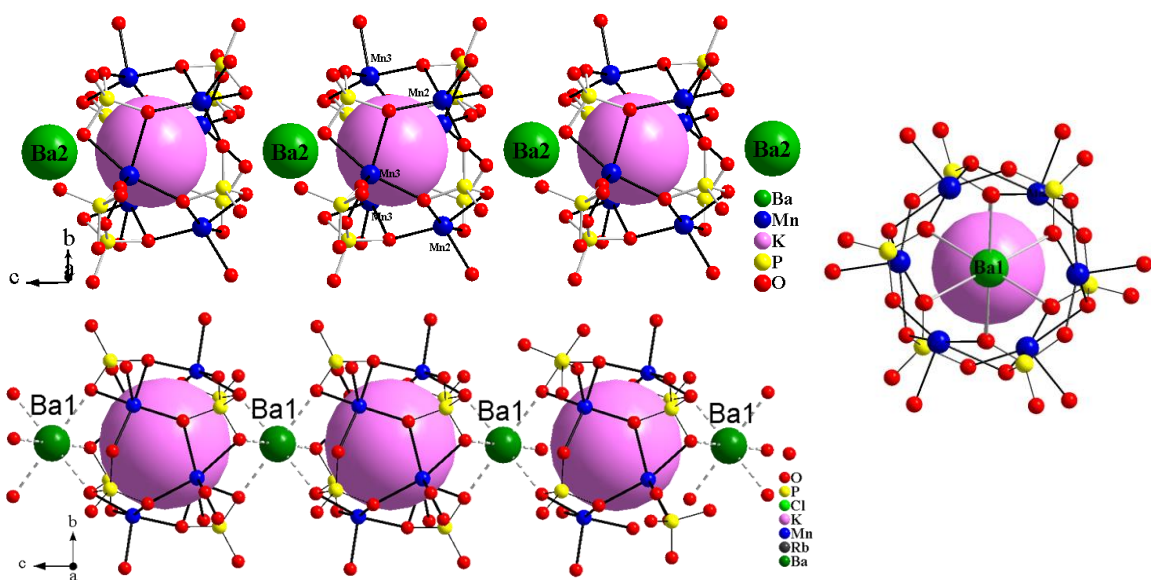
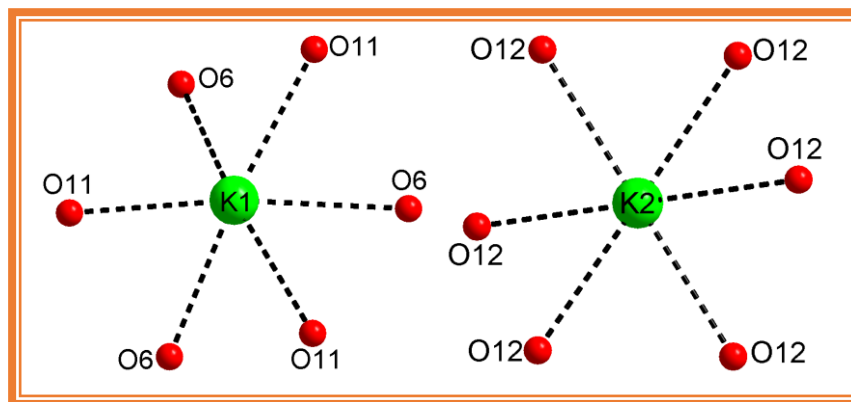


Figure 7. The partial structure showing potassium ions residing in the middle of $\text{Mn}_6(\text{PO}_4)_6$ units and barium ions residing in between the $\text{Mn}_6(\text{PO}_4)_6$ units (left). The $\text{Mn}_6(\text{PO}_4)_6$ unit together with barium cations capping both sides to form a cage for potassium ions to reside in (right).

Table 8. Selected Bond Distances (\AA) in KO_6 units and Bond valence sum

Bond	Bond length (\AA)	Valence K^{I}
K(1)-O(11) ^{xv}	3.176(7)	0.059
K(1)-O(11) ^{xvi}	3.176(7)	0.059
K(1)-O(11) ^{xvii}	3.176(7)	0.059
K(1)-O(6) ^{xvi}	3.234(7)	0.050
K(1)-O(6) ^{xv}	3.234(7)	0.050
K(1)-O(6) ^{xvii}	3.234(7)	0.050
	Sum	0.33
K(2)-O(12) ^{xi}	3.321(7)	0.04
K(2)-O(12) ^v	3.321(7)	0.04
K(2)-O(12)	3.321(7)	0.04
K(2)-O(12) ^{ix}	3.321(7)	0.04
K(2)-O(12) ⁱⁱⁱ	3.321(7)	0.04
K(2)-O(12) ^{xviii}	3.321(7)	0.04
	Sum	0.24

K(1)O₆ and K(2)O₆ Polyhedra**Figure 8.** Coordination environment around around potassium cations.

The bond valence sum (BVS) calculations^{17,18} based upon observed distances are consistent with the assigned formal oxidation states of the cations; the calculated valences for $K^{1+}(1)$ and $K^{1+}(2)$ cations are +0.33 v.u. and +0.24 v.u., respectively as shown in Table 8. Based on the factors discussed above we can conclude that ideal Ba-O occurs but there is a less likelihood that bonding occurs between potassium and oxygen and it turns out that potassium cations seemingly rattle inside the cages due to loosely bonded potassium and oxygen.

As shown in Figure 9, corner sharing MnO_5 square pyramids and PO_4 tetrahedra sharing edges and corners with MnO_5 square pyramids form an extended structure leaving one dimensional channel structure with two types of channels where barium and potassium cations reside in one channel while rubidium cation sits in the other. The rubidium cations are situated in the middle of a channel surrounded by three other channels. The two crystallographically independent rubidium cations reside in a RbO_9 environment that can be seen in Figure 9 and the dotted lines indicate longer Rb-O bonds.

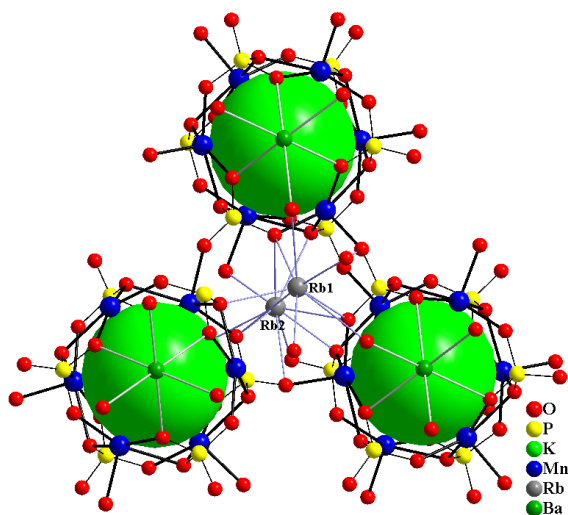


Figure 9. The corner-sharing PO_4 tetrahedra and MnO_5 square pyramids form a pseudo one dimensional channel structure with two types of channels where barium and potassium cations reside in one channel while rubidium cation sits in the other.

As shown in Table 9, The Rb–O bond distances range from 2.719 (7) Å to 3.450 (8) Å. The average Rb-O distances in Rb(1)-O and Rb(2)-O are 2.98 Å and 2.98 Å, respectively, which are comparable with the sum of Shannon crystal radii (2.98 Å) of nine coordinate Rb^+ (1.77 Å) and O^{2-} (1.21 Å)^{17,18}. Taking into account all the Rb-O bonds, the calculated valences for $\text{Rb}^{1+}(1)$ and $\text{Rb}^{1+}(2)$ cations are +1.49 vs. and +1.51 v.u., respectively as shown in Table 9. In addition to that calculated valences for $\text{Rb}^{1+}(1)$ and $\text{Rb}^{1+}(2)$ cations based upon distances below 3.00 Å are +1.14 and +1.03, respectively. Thus, we can agree with the fact that all the rubidium ions in this compound are in +1 oxidation states. The final values resulted from Bond-valence sum (BVS) calculations for the title compound can be summarized as +1.93, +1.94, +1.91, +4.95, +4.99, +2.02, +1.87, +1.14, and +1.03 valence units for Mn(1), Mn(2), Mn(3), P(1), P(2), P(3), Ba(1), Ba(2), Rb(1), and Rb(2), respectively, which in each case is close to the expected values of 2 for Mn, 5 for P, 2 for Ba, and 1 for Rb. The summery of Bond-valence sum (BVS) calculations for all the ions is given in the Table 10.

The BVS around the K^+ ions are only 0.33 v.u. and 0.24 v.u. much smaller than the expected 1.0. Therefore, on can conclude that the K^+ ions do not appear to be in contact with any other atom firmly. The large variation in the K-O distance is understandable in terms of the BVS. It has been reported that even in a complex with only two different types of bonds, there are many combinations of expansions of one bond or the other that would cause the BVS to decrease by 1.0 from a giving starting point.⁴⁴ It is interesting to notice that potassium cations seemingly rattle inside the cages due to loosely bonded potassium and oxygen.

Table 9. Selected Bond Distances (Å) in RbO₉ units and Bond valence sum

Bond	Bond length (Å)	Valence Rb ^I	Bond	Bond length (Å)	Valence Rb ^I
Rb(1)-O(1) ^{vii}	3.349(7)	0.053	Rb(2)-O(10) ^{xii}	2.686(7)	0.32
Rb(1)-O(2)	2.742(7)	0.27	Rb(2)-O(6)	2.719(7)	0.29
Rb(1)-O(3)	2.777(7)	0.25	Rb(2)-O(7) ^{vi}	2.725(7)	0.24
Rb(1)-O(4)	2.795(7)	0.24	Rb(2)-O(11) ^{xiii}	2.908(7)	0.17
Rb(1)-O(12)	2.840(7)	0.21	Rb(2)-O(10) ^{xiv}	3.035(7)	0.12
Rb(1)-O(5)	2.908(7)	0.17	Rb(2)-O(9)	3.063(8)	0.11
Rb(1)-O(2) ^x	3.070(7)	0.11	Rb(2)-O(5) ^{vi}	3.110(8)	0.10
Rb(1)-O(8) ^{xi}	3.101(7)	0.10	Rb(2)-O(3) ^{vi}	3.115(8)	0.099
Rb(1)-O(7)	3.202(9)	0.079	Rb(2)-O(4)	3.450(8)	0.040
	Sum	1.49		Sum	1.51

Symmetry transformations used to generate equivalent atoms: (i) $-x, -y+2, -z+2$; (ii) $y-1, -x+y, -z+2$; (iii) $-y+1, x-y+2, z$; (iv) $x-y+1, x+1, -z+2$; (v) $-x+y-1, -x+1, z$; (vi) $x, y, z-1$; (vii) $-y+1, x-y+1, z$; (viii) $-x+y, -x+1, z$; (ix) $y-1, -x+y, -z+3$; (x) $-x+1, -y+2, -z+3$; (xi) $x-y+1, x+1, -z+3$; (xii) $y, -x+y+1, -z+3$; (xiii) $-x+1, -y+2, -z+2$; (xiv) $-x+y, -x+1, z-1$; (xv) $-y+1, x-y+1, z+1$; (xvi) $x, y, z+1$; (xvii) $-x+y, -x+1, z+1$; (xviii) $-x, -y+2, -z+3$; (xix) $x-y+1, x, -z+3$; (xx) $-y+1, x-y+1, z-1$.

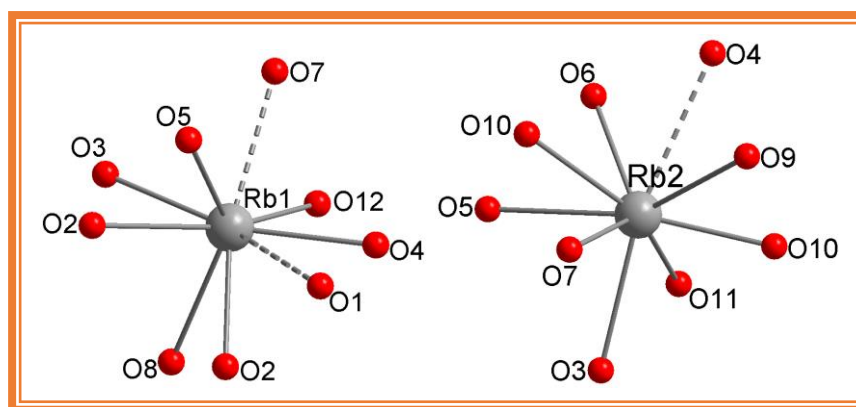
Rb(1)O₉ and Rb(2)O₉ Polyhedra**Figure 10.** Drawings of RbO₈ polyhedra. The dotted lines represent long Rb-O bonds.

Table 10. The summary of Bond valence sum

Atom	Coordination Number	Oxidation Number	Cation	BVS
Mn(1)	5	2	Mn ^{II}	1.93
			Mn ^{III}	1.78
Mn(1)	5	2	Mn ^{II}	1.94
			Mn ^{III}	1.79
Mn(1)	5	2	Mn ^{II}	1.91
			Mn ^{III}	1.76
P(1)	4	5	P ^{III}	5.12
			P ^V	4.95
P(2)	4	5	P ^{III}	5.15
			P ^V	4.97
P(3)	4	5	P ^{III}	5.17
			P ^V	4.99
Ba(1)	6	2	Ba ^{II}	2.02
Ba(2)	6	2	Ba ^{II}	1.87
K(1)	6	1	K ^I	0.33
K(2)	6	1	K ^I	0.24
Rb(1)	9	1	Rb ^I	1.49
Rb(2)	9	1	Rb ^I	1.51

According to our structural study, the title compound has an open framework showing different tunnels, contain different disordered cations with possible relatively thermally agitations. These factors promote ionic conductivity which prompts one to study the alkali-ions pathways simulation in the title compound. The transport pathways modeling of K, Rb,

and Ba cations in the anionic framework can be carried out using the BVSE simulation model based on the crystallographic data of the studied materials.⁴⁵

The structure of the title compound generated based on the crystallographic data (Table 2) by placing the atoms of three formula units (as shown in Table 1) into the box which represents the unit cell. Knowledge of the crystal structure implies that we are able to describe the unit cell of the compound. The unit cell is a structural component that, when repeated in all directions, result in a macroscopic crystal. Figure 11 represents the unit cell of the title compound showing a space-filling representation which reveals the regular arrangements of Ba, Rb, K, Mn, P, and O atoms. In order to determine the chemical formula for this phase given the crystal structure, it is required to count all sorts of atoms inside the unit cell, taking into account fractional atoms (that is account for shared atoms) and adjust so that ratios going to be integers. For example, an atom at the corner of the unit cell counts as 1/8 atom because it is shared between 8 adjacent unit cells.

Likewise, an atom at the edge of the unit cell counts as 1/4 as it belongs to 4 unit cells, and an atom at the phase of the unit cell counts as 1/2 as it belongs to 2 unit cells. In order to obtain fractional values for the atom numbers, it is required to multiply the values of all the atoms with a certain number so that all values are integers. There are four types of sites in the unit cell of the title compound: unique central position (some of the Ba, Rb, K, Mn, P, and O ions belong entirely to the unit cell); face site (some of the Rb and O ions are shared between two unit cells); edge sites (some of the Rb and K ions the ion is shared between four unit cells); corner site (some of the Ba ions are shared between eight

unit cells). As shown in Table 12, the total number of Ba, Rb, K, Mn, P, and O atoms belonging to the unit cell can be calculated and the ratio of Ba : Rb : K : Mn : P : O is 3:9:3:18:18:72. The fact that one can determine the empirical formula of a compound if we know the mole ratio of the elements enables us to identify the compound theoretically. Thus, the empirical formula tells us which elements are present and the simplest whole-number ratio of their atoms.

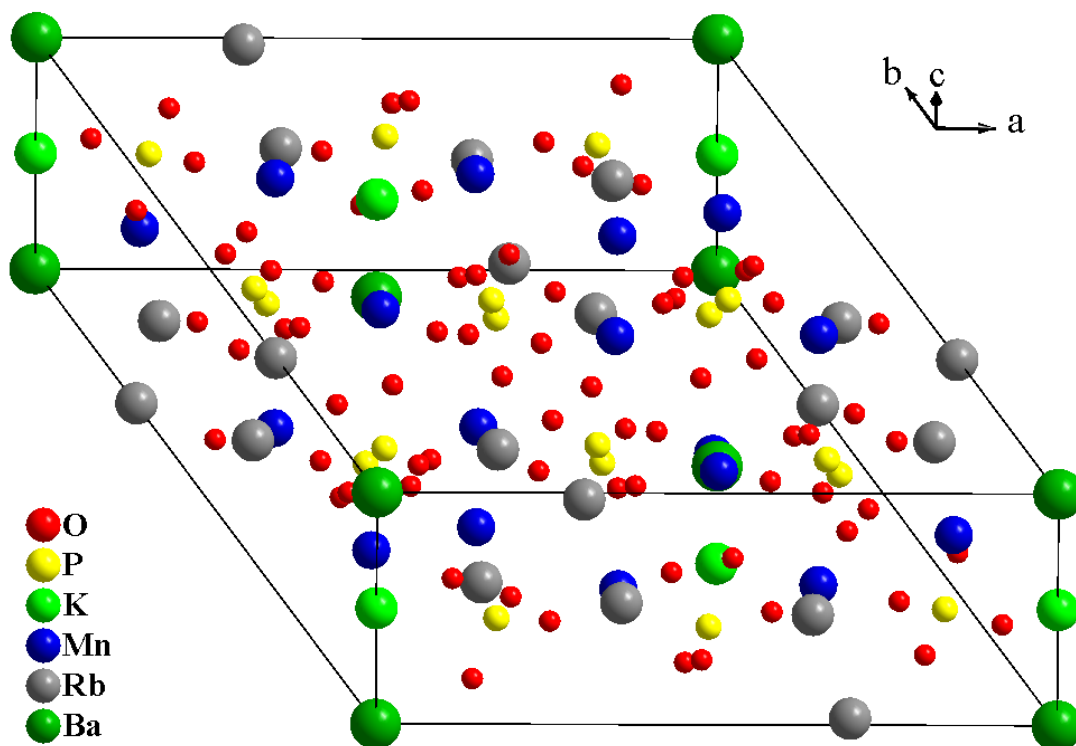


Figure 11. The representations of the unit cell of the compound showing a space-filling representation which reveals the regular arrangements of Ba, Rb, K, Mn, P, and O atoms in three dimensions where the metal lattice arrange themselves in a certain pattern which can be represented as a 3D box structure. The Ba ions are shown in green, Rb ions are shown in gray, K ions are shown in light green, Mn ions are shown in blue, P ions are shown in yellow, and the O ions are shown in red. There are four types of sites in the unit cell: central, face, edge, and corner positions.

Table 12. Number of atoms per unit cell in the title compound.

Site	Ba	Rb	K	Mn	P	O
Central	2	2	2	18	18	68
Phase	0	$10*(1/2) = 5$	0	0	0	$8*(1/2) = 4$
Edge	0	$8*(1/4) = 2$	$4*(1/4) = 1$	0	0	0
Corner	$8*1/8 = 1$	0	0	0	0	0
Total	3	9	3	18	18	72

It suggests that the structure of the unit cell for this compound is consistent with the formula, $\text{BaRb}_3\text{KMn}_6(\text{PO}_4)_6$ and it also implies that there are three formula units per unit cell as indicated in Table 12.

According to the overall formula of $\text{BaRb}_3\text{KMn}_6(\text{PO}_4)_6$, based on the final values resulted from Bond-valence sum (BVS) calculations, +1.93, +1.94, +1.91, +4.95, +4.99, +2.02, +1.87, +1.14, and +1.03 valence units for Mn(1), Mn(2), Mn(3), P(1), P(2), P(3), Ba(1), Ba(2), Rb(1), and Rb(2), respectively, the manganese atoms should adopt a di-valence state where Mn(1), Mn(2), and Mn(3), are Mn^{2+} and the phosphorous atoms should adopt a penta-valence state where P(1), P(2), and P(3) are P^{5+} to balance the overall charge so that $\text{BaRb}_3\text{KMn}_6(\text{PO}_4)_6$, can be formulated as $\text{Ba}^{\text{II}}\text{Rb}^{\text{I}}_3\text{K}^{\text{I}}\text{Mn}^{\text{II}}_6(\text{P}^{\text{V}}\text{O}_4)_6$. Transition metal such as manganese in coordination compounds can adopt different oxidation states. Employing Bond Valence Sum (BVS) model, based solely on structural information, we were able to relate the bond lengths around a metal center to its oxidation

state and assigned the oxidation state, +2 for manganese atoms. Our calculations provide details on the oxidation states of the metal ions and serves as an additional support for the accuracy of the determination of empirical formula. This imply that The BVS analysis is a relatively simple calculation that can be carried out for many other transition metal oxides. Its powerful ability for the determination of oxidation states of manages and phosphorous atoms in $\text{BaRb}_3\text{KMn}_6(\text{PO}_4)_6$ has been demonstrated unambiguously. Although BVS analysis has not been applied routinely, we hope this work will encourage other students to begin the employment of this tool to obtain a better understanding of their interest in transition metal oxides.

Conclusions

The BVS analysis has been widely applied to problems in coordination chemistry, particularly in the assignment of oxidation states and also in validating the crystal structure determinations by comparing the valences of the atoms with the sums of their experimental bond valences. Its powerful ability for the determination of oxidation states of metal ions has been demonstrated for the $\text{BaRb}_3\text{KMn}_6(\text{PO}_4)_6$ compound. We found that the longer bond distances in K-O and Rb-O were indicated by the values calculated by BVS that have deviated significantly from the expected value so that a closer look at the structure determination was initiated together with placing the atoms of three formula units into the unit cell. The BVS is a relatively simple calculation if the appropriate R_0 values are available. For the Mn case with O donor atoms, we have shown that the regardless of the employment of an R_0 of 1.790 Å or 1.760 Å still correct oxidation state

for the Mn atoms could be determined. The results are in good agreement for oxidation states of Mn(II) and P(V). The agreement with K(I) was not very good, which may be a reflection of unusually longer bonds and coordination environment. Usually the deviation of the BVS from an integer value usually indicates problems with the structure but taking into account our analysis of the structure of based on the crystallographic data by placing the atoms of three formula units into the unit cell. It turned out that the manganese and barium atoms should adopt a di-valence state, phosphorous atoms should adopt a penta-valence state, and rubidium and potassium atoms should adopt a mono-valence state to balance the overall charge so that $\text{BaRb}_3\text{KMn}_6(\text{PO}_4)_6$, can be formulated as $\text{Ba}^{\text{II}}\text{Rb}^{\text{I}}_3\text{K}^{\text{I}}\text{Mn}^{\text{II}}_6(\text{P}^{\text{V}}\text{O}_4)_6$. In cases where the ligand oxidation state is ambiguous, the BVS can be used as a guide for the oxidation state of the metal. The BVS can be extremely useful to chemists in evaluating the results of a crystal structure analysis or in resolving conflicts regarding oxidation states. Structural chemists should be able to utilize the BVS to support the crystal structure analysis. The concept can be applied regarding the oxidation state and can help prevent serious errors prior to publication.

LITERATURE CITED

1. Brown, I. D. *The Chemical Bond in Inorganic Chemistry, The Bond Valence Model*. Oxford University Press: Oxford, **2002**.
2. Housecroft C, Sharpe A.G. *Inorganic Chemistry*, 4th Ed.: Pearson Education: Essex, **2012**.
3. Nguyen, Tu N. *ChemRxiv*. **2020**, 1-10.
4. Smith, D. W. *J. Chem. Educ.* **2005**, 82, 1202–1204.
5. Parkin, G. *J. Chem. Educ.* **2006**, 83, 791–799.
6. West, A. R. *Basic Solid State Chemistry*, John Wiley & Sons: New York, 2000.
7. Pauling, L. *J. Am. Chem. Soc.* **1929**, 51, 1010-1026.
8. Bragg, W. L. *Z. Kristallogr.* **1930**, 74, 237-305.
9. Preiser, C.; Loßel, J.; Brown, I. D.; Kunz, M.; Skowron, A. *Acta Crystallogr.* **1999**, B55, 698-711.
10. Brown, I.D. *Chem. Rev.* **2009**, 109, 6858–6919.
11. Baur, W. H. *In Structure and Bonding in Crystals*, Vol. II; O’Keeffe, M., Navrotsky, A., Eds.; Academic Press: London, 1981; Chapter 31
12. Donnay, G.; Allmann, R. *Am. Mineral.* **1970**, 55, 1003-1015.
13. Pauling, L. *J. Am. Chem. Soc.* **1947**, 69, 542-553.
14. Zachariasen, W. H. *Acta Crystallogr.* **1954**, 7, 795-799.
15. Mohri, F. *Acta Crystallogr.* **2000**, B56, 626-638.
16. Etxebarria, I.; Perez-Mato, J. M.; Garcia, A.; Blaha, P.; Schwarz, K.; Rodriguez-Carvajal, J. *Phys. Rev. B* **2005**, 72, 174108-174116.
17. Brown, I. D.; Altermatt, D. *Acta. Crystallogr.* **1985**, B41, 244-247.
18. Brese, N. E.; O’Keeffe, M. *Acta Crystallogr.* **1991**, B47, 192-197.

19. Allen, F. H. *Acta Cryst.* **2002**, *B58*, 380–388.
20. Groom, C. R.; Bruno, I. J. ; Lightfoot, M. P. ; Ward, S. C. *Acta Cryst.***2016**, *B72*, 171–179.
21. Bergerhoff, G.; Brandenburg, K. *International Tables for Crystallography*, Vol. C, edited by J. C. Wilson & E. Prince, Kluwer Academic Publishers: Dordrecht, 2004; pp. 778–789.
22. Shields, G. P.; Raithby, P. R.; Allen, F. H.; Motherwell, W. D. S. *Acta Cryst.* **2000**, *B56*, 455–465.
23. Trzesowska, A., Kruszynski, R. & Bartczak, T. J. *Acta Cryst.* **2004**, *B60*, 174–178.
24. Trzesowska, A., Kruszynski, R. & Bartczak, T. J. *Acta Cryst.* **2006**, *B62*, 745–753.
25. Shannon, R. D.; Prewitt, C. T. *Acta Crystallogr.* **1969**, *B25*, 925-946.
26. Shannon, R. D. *Acta Crystallogr. Sect. A.* **1976**, *32*, 751-767.
27. Nag, S.; Banerjee, K.; Datta, D. *New J. Chem.* **2007**, *31*, 832-834.
28. Zheng, H.; Langner, K.M.; Shields, G.P.; Hou, J.; Kowiel, M.; Allen, F.H.; Murshudov, G.; Minor, W. *Acta Crystallogr. Sect. D.* **2017**, *73(4)*, 316–325.
29. Brown, I. D. *Acta Crystallogr. Sect.B.* **1992**, *B48*, 553-572.
30. O’Keeffe, M. *Acta Crystallogr. Sect. A.* **1990**, *A46*, 138-142.
31. Brown, I. D. 2008. http://www.ccp14.ac.uk/ccp/web-mirrors/i_d_brown.
32. Adams, S. 2008, <http://www.softBV.net>.
33. Wills, A. S. http://www.chem.ucl.ac.uk/people/wills/bond_valence/bond_valence.html.
34. Shields, G. P.; Raithby, P. R.; Allen, F. H.; Motherwell, W. D. S. *Acta Crystallogr.* **2000**, *B56*, 455-465.
35. Allen, F. H.; Davies, J. E.; Galloy, J. J.; Johnson, O.; Kennard, O.; Macrae, C. F.; Mitchell, F. M.; Mitchell, G. F.; Smith, J. M.; Watson, D. G. *J. Chem. Inf. Comput. Sci.* **1991**, *31*, 187-204.
36. Cramer, S. P.; Hodgson, K. O. *Prog. Inorg. Chem.* **1979**, *25*, 1-40.

37. Thorp, H. H. *Inorg. Chem.* **1992**, *31*, 1585-1588.
38. Liu, W.; Thorp, H. H. *Inorg. Chem.* **1993**, *32*, 4102-4105.
39. Wells, A. F. *Structural Inorganic Chemistry*, 5th ed.; Oxford University Press: New York, **1984**.
40. Cotton, F. A.; Wilkinson, G. *Advanced Inorganic Chemistry*; 4th ed.; Wiley: New York, **1980**.
41. Nhat, H. N. Los Alamos National Laboratory, Preprint Archive, *Condensed Matter* **2003**, 1-11. <https://arxiv.org/abs/cond-mat/0308610>.
42. Sheldrick, G. M. In "SHELXTL, Version 6.1 Structure Determination Software Programs; Bruker Analytical X-ray Systems Inc., Madison, WI, **2001**.
43. *Diamond*: v. 2.1, Brandeuburg, K 1999.
44. Thorp, H. H. *Inorg. Chem.* **1998**, *37*, 5690-5692.
45. Adams, S.; Swenson, J. *Phys. Rev. Lett.* **2000**, *84*, 4144-4147.